Langmuir Circulations in a Surface Layer Bounded by a Strong Thermocline

STEPHEN M. COX* AND SIDNEY LEIBOVICH

Sibley School of Mechanical and Aerospace Engineering, Cornell University, Ithaca, New York

(Manuscript received 13 December 1991, in final form 2 July 1992)

ABSTRACT

Langmuir circulations reside in, and are responsible in part for the existence and maintenance of, the mixed layer. It is, therefore, typical for the water containing Langmuir circulations to be bounded below by a thermocline. When this bounding thermocline is strong, it may be expected to act as an effective "slippery bottom" constraint. Such an assumption has been invoked previously, but failed to predict a preferred spacing for the windrows produced by the circulations. This model assumed that the momentum transfers across the horizontal boundaries of the mixed layer were independent of the water motion induced by Langmuir circulation. Here, mixed boundary conditions are explored. Estimates of the transfer coefficients in these boundary conditions suggest that the revised model differs only slightly from the earlier one, but allows for a more general and realistic stress model. Incorporating these effects into the theory gives windrows with a finite separation, in accord with the observations. The windrow spacing emerging from this modified theory depends in a simple way on the layer depth and the constant of proportionality in the stress boundary condition when the latter number takes physically plausible values. The analysis allows the water layer above the bounding thermocline to be homogeneous or either stably or unstably density stratified. The stably stratified case permits oscillatory convection under certain restricted circumstances.

1. Introduction

Observational evidence shows that Langmuir circulation may have a range of coexisting length scales, the largest of which seems to be related to the depth of the principal thermocline. This indicates that the existence of a strong thermocline inhibits convective activity and acts as an effective bottom for Langmuir circulations. The idea that the pycnocline establishes the effective depth of the circulations was first put forward by Langmuir (1938), and it is consistent with linear stability theory (see Leibovich 1977b). The mathematical treatment of motion in a finite layer is much simpler than in a body of water that is modeled as infinite in depth, and is easier to treat in computer studies. With these points in mind, several recent papers (Leibovich 1985; Moroz and Leibovich 1985; Leibovich et al. 1989; Cox et al. 1992a,b) have considered a model of a horizontally infinite layer of finite depth subjected to constant applied horizontal stress at both top and bottom (abbreviated hereafter by CSM, for "constant stress model"). The basis for these papers is the theory (hereafter CL) of Langmuir circulations developed by Craik and Leibovich (1976), Craik (1977), and Leibovich (1977a,b, 1980), which shows how the rectified effects of small-amplitude surface gravity waves may destabilize wind-driven currents. The theory allows for nonlinear equilibration in the form of convective motions having as their preferred form a system of vortical rolls with axes parallel to the wind direction. Windrows are the surface manifestations of this roll system.

Our intent here is to take a step toward realism by focusing on important consequences that follow from choices made in modeling boundary conditions. No claim is made to full incorporation of all physical effects that come into play, even within the specific context of the CL theory.

Various boundary conditions may be appropriate to the CL theory. Requiring constant stress at the boundaries implies that the stress perturbations vanish there. This choice of boundary condition turns out not to shed light on the preferred spacing of windrows and underlying cells, at least on linear grounds, because modes of infinite wavelength are the first to be destabilized. This is also found to be the case in thermal convection with thermally insulating boundaries (Sparrow et al. 1964; Nield 1967) and in related problems. The inclusion of nonlinear effects appears to provide no remedy, since numerical evidence offered by Chapman and Proctor (1980) shows that initial data

* *Current affiliation:* Department of Applied Mathematics, The University of Adelaide, South Australia.

Corresponding author address: Dr. Sidney Leibovich, Dept. of Mechanical & Aerospace Engineering, 248 Upson Hall, Cornell University, Ithaca, NY 14853-7501.

with finite wavelength cascade to larger and larger scales. This nonlinear cascade is remarkable, because for unstable conditions the mode that grows most rapidly according to linear theory has a *finite* wavelength.

Of course, the CSM fails to reflect the coupling of the perturbed motion and the extra stress it must produce. Thus, the CSM, and especially the assumption of vanishing perturbation stress at the base of the mixed layer, is associated with some degree of error in modeling the physics. Here, we try to improve on the CSM by allowing for the omitted coupling, with attention focused on the assumption that the motion is independent of the coordinate in the direction of the wind. In the model explored here, we assume that the wind speed, rather than the stress transmitted to the water, is held fixed, and the current speed below the pycnocline, rather than the stress at the base of the mixed layer, is also held fixed. Under certain assumptions, this leads to mixed boundary conditions that turn out, in contrast to the CSM, to predict a finite windrow spacing based on linear stability grounds.

The coupling effects are estimated to be moderately small. We attempt to exploit this by exploring the asymptotic limit as the coupling becomes extremely small. This proves to be advantageous, because in this limit, the horizontal wavelength of the marginally stable linear mode is very long. With this fact as guidance, we are able to construct a fully nonlinear model similar to those produced in related physical problems (see Chapman and Proctor 1980; Sivashinsky 1982, 1983). Arguments based on the fully nonlinear theory confirm the finite windrow spacing indicated by the linear stability results. Observations by Smith et al. (1987) reveal large-scale Langmuir circulation with a windrow spacing approximately three times the mixed-layer depth, thus having a wavenumber of about 2, measured in units of inverse mixed-layer depth. The long-wave limit is not an accurate representation of these circumstances. The small-wavelength analysis nevertheless interests us for three reasons. First, the observational methods become increasingly inaccurate as the length scale of the circulation increases and are unable to detect extremely large scales if they are present. Second, the consequences of the long-wave assumption allow us to make considerable analytical progress, and at the same time, comparisons with exact numerical calculations show that the long-wavelength approximation is accurate for wavenumbers that are not small compared to 1. Consequently, one might be prepared to accept the asymptotic estimates as a guide even where the formal conditions for the analysis are not satisfied. Third, the results of the simple asymptotic analysis contain features, such as cascades from small to large scales, that have been associated with observational reports of Langmuir circulation.

In previous theoretical treatments, the thermal boundary conditions were taken to be either constant temperature, or constant heat flux. One might think that modifications of the thermal boundary conditions rather than the mechanical ones would provide a preferred wavenumber, but this turns out not to be true. In this paper, we explore the effects of more general thermal boundary conditions than we have previously admitted in our theoretical studies on Langmuir circulation. These boundary conditions are physically more realistic and allow for variations in surface temperature as well as spatial and temporal variations in heat flux. In most cases, the qualitative nature of the circulations is unaffected, but in a restricted set of circumstances with the thermal exchanges permitted here at the boundaries, the convection becomes oscillatory in time rather than steady.

Provided that the surface gravity wave field produces a Stokes drift having a depth that is not small compared to the depth of the mixed layer, the conclusion here is that the preferred spacing of windrows is large compared to the layer depth, with a weak dependence on the exchange coefficient characterizing the stress boundary condition. In the event that the dominant waves are short compared to the layer depth, the analysis here does not apply, and the problem must be reconsidered.

We describe the situations of interest in section 2, giving particular attention to the boundary conditions and to estimates of the parameters that appear in them. A dimensionless statement of the full mathematical problem for two-dimensional Langmuir circulations according to the CL theory is given in the next section. Instability thresholds and growth rates according to linear stability theory are given in section 4; the algebraic details that lead to these results are given in the Appendix. Although the description of the instability found here is similar to that found by Chapman and Proctor (1980) for thermal convection, and by Sivashinsky (1982, 1983) for Marangoni convection, there are more cases to be considered. In particular, none of the previous papers permitted a mixed boundary condition in more than one dependent variable, while here this is permitted for two (thermal and stress boundary conditions). This leads to complexities not encountered in the previous work, and the new possibility of oscillatory convection is found. Nonlinear evolution equations, valid without restriction on the *magnitude* of the disturbance levels, are given in section 5 for the cases where linear stability theory predicts bifurcation to steady convection. The detailed results are given for the case of exponentially decaying Stokes drift, but the form and general conclusions are expected to stand for an arbitrary Stokes drift, provided it has a monotonic decay with depth. The remaining case, the nonlinear evolution of oscillatory convection, is not discussed. The results of sections 4 and 5 are discussed in section 6, where we present diagrams to illustrate the Langmuir circulation cells in the extreme cases of short and long surface gravity waves. A summary of our results is given in section 7.

2. Problem specification

a. Boundary conditions

To fix our problem, we suppose that the wind at some "anemometer" height above the mean water surface is constant in speed and in direction, which we take to coincide with the x axis. A strong thermocline exists at a depth d below the mean water surface, $z = 0$, and the water above it is either of uniform density, or stratified with a modest density gradient. It is supposed that the thermocline is strong enough to prevent the penetration of any significant convective motion, so that the plane $z = -d$ acts like an impenetrable surface. The water below the thermocline may be moving. If so, its horizontal speed, like that of the wind, is supposed constant in speed and direction with x and y components of u_{below}, v_{below}, respectively.

A stress will be exerted on the water, some of which will provide the momentum radiated away from the local water column by surface waves, and the residual will increase the momentum of the local current system. We suppose that the surface waves are statistically stationary and horizontally homogeneous and that the associated Stokes drift is rectilinear with speed $U_S(z)$ in the wind direction. Furthermore, we suppose that the wind speed U_a has been discounted for any momentum transferred to the waves, so that only the stress that transfers momentum to the current system is accounted for. The mean surface water speeds are much smaller than the wind speed at standard anemometer heights, typically by a factor of 30 or so, and so the usual practice in estimating the stress applied to the water surface is to ignore the surface current speed. In this approach, a constant value of U_a implies a constant applied stress. This is a good approximation, but there are clearly small departures from it due to a number of factors.

To begin with, imagine a (nonphysical) situation in which (through the action of some genie) the surface remains plane when the wind blows. Let the stress vector be $\boldsymbol{\tau}$. Assume a constant bulk momentum exchange coefficient, C_m, and fix the stress vector applied to the water surface by the wind to be

$$\boldsymbol{\tau} = C_m \rho_a \sqrt{(U_a - u_s)^2 + v_s^2}\,[(U_a - u_s)\mathbf{i} - v_s \mathbf{j}], \quad (1)$$

where u_s and v_s are the components of the mean surface water current in the x (windward, unit vector $\mathbf{i}$) and y (crosswind, unit vector $\mathbf{j}$) directions, respectively, and ρ_a is the air density. The water-current speed is small compared to U_a, so we can approximate (1) by

$$\boldsymbol{\tau} \approx \rho_w u_*^2 \left[\left(1 - 2\frac{u_s}{U_a}\right)\mathbf{i} - \frac{v_s}{U_a}\,\mathbf{j}\right],$$

where ρ_w is the water density, and u_* is the *water* friction velocity defined here by $\rho_w u_*^2 = C_m \rho_a U_a^2$. This leads to the surface stress boundary conditions

$$\frac{\boldsymbol{\tau}\cdot\mathbf{i}}{\rho_w u_*^2} + \frac{2u_s}{U_a} = 1,$$

$$\frac{\boldsymbol{\tau}\cdot\mathbf{j}}{\rho_w u_*^2} + \frac{v_s}{U_a} = 0. \quad (2)$$

Invoking an eddy viscosity, ν_T, we may express the stress at the boundaries as

$$\frac{\boldsymbol{\tau}}{\rho_w} = \nu_T \frac{\partial \mathbf{v}}{\partial z} \quad \text{at} \quad z = 0, -d,$$

and then (2) takes the form

$$\frac{\nu_T}{u_*^2}\frac{\partial \mathbf{u}}{\partial z} + \mathbf{B}\cdot\mathbf{u} = \mathbf{i}, \quad (3)$$

where the diagonal matrix $\mathbf{B}$ is

$$\mathbf{B} = \begin{pmatrix} B_1 & 0 \\ 0 & B_2 \end{pmatrix} = \frac{1}{U_a}\begin{pmatrix} 2 & 0 \\ 0 & 1 \end{pmatrix}.$$

The mixed boundary condition (3) leads to a reduction of the stress as the surface current increases at fixed wind speed. This is simplistic, however, since a significant part of the stress transferred is due to momentum transfer from breaking waves. As the surface current increases, the wave breaking increases as well, so a larger fraction of the surface wave spectrum is liable to breaking (cf. Phillips 1977). Increased wave breaking offsets the stress reduction, perhaps even leading, under some conditions, to a stress *increase.* Nevertheless, it is not unreasonable to model the stress by a boundary condition of mixed type as in (3), but with $\mathbf{B}$ a diagonal matrix with different, perhaps even negative, elements.

Similar conditions may be applied, again admittedly somewhat speculatively, to couple the mixed layer to the water below it. Current speeds typically are much smaller below the pycnocline than they are just above it. The higher effective viscosity in the turbulent (or simply the convective) motion in the mixed layer is one way to think of the cause of the boundary-layer character exhibited across the thermocline. The momentum flux from the mixed layer to the water below is modeled here in a way that has been suggested for integral models of the mixed layer (Niiler and Kraus 1977). The two transfer mechanisms contemplated are due first to entrainment at the base of the mixed layer, with an entrainment velocity, w_e, to be specified, and second to downward radiation of momentum in internal waves (Pollard and Millard 1970). Niiler and Kraus (1977) suggest parameterization of this effect by means of a constant drag coefficient. We note that if the depth of the mixed layer remains constant, then any time-independent horizontally averaged current that may emerge must have the stress imposed at the surface balanced by the stress imposed at the bottom, and with the mechanisms suggested here, this implies

that the stress is imposed by internal wave radiation. Accordingly, we will take the contribution of the internal wave drag in the form $\rho_w[mu_*^2\mathbf{i} + C_{IW}u_*(\Delta u\mathbf{i} + \Delta v\mathbf{j})]$. Here we have taken $\Delta u \equiv u_{\text{bottom}} - u_{\text{below}}$ and $\Delta v \equiv v_{\text{bottom}} - v_{\text{below}}$ to be the difference of the horizontal velocity components at the bottom of the mixed layer (i.e., as $z \downarrow -d$) and the corresponding velocity components in the fixed current below the mixed layer; the "extra" wave stress has been taken in the form of a linear friction. Figure 1 summarizes some of the notation introduced in this section.

The dimensionless parameter m is a measure of the fraction of the stress attributable to internal waves. When the mixed layer has constant depth and is in dynamical equilibrium, then all of the stress at the bottom is accounted for by internal wave radiation, and m approaches one.

The bottom stress boundary conditions, allowing for entrainment and radiation, are

$$\frac{\nu_T}{u_*^2}\frac{\partial u}{\partial z} = \left(\frac{w_e}{u_*} + C_{IW}\right)\frac{\Delta u}{u_*} + m,$$

$$\frac{\nu_T}{u_*^2}\frac{\partial v}{\partial z} = \left(\frac{w_e}{u_*} + C_{IW}\right)\frac{\Delta v}{u_*}, \qquad (4)$$

at $z = -d$. In the next subsection, we shall estimate the entrainment velocity based on the overall Richardson number across the pycnocline using the experimental data discussed by Phillips (1977).

Whenever a nonzero entrainment velocity is invoked, we must allow the mixed-layer depth, d, to change with time (since $\dot{d} = w_e$). In the stability analysis to follow, we suppose that any such changes are much slower than the time scales for Langmuir circulation instability to occur, so that the depth variations may be treated quasi statically.

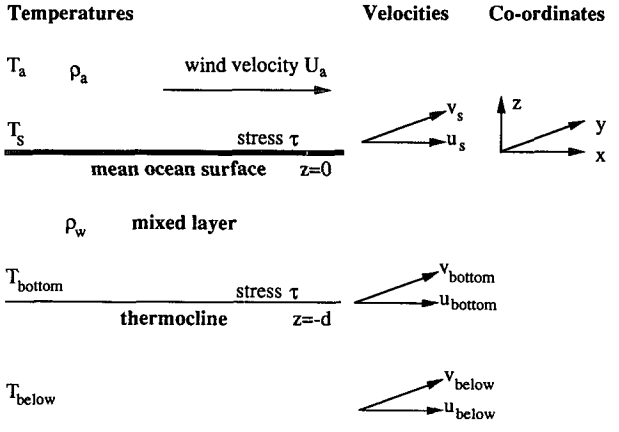

FIG. 1. A summary of the notation we have used in section 2a. The subscript a refers to quantities associated with the air above the ocean surface; s to quantities associated with the ocean at its surface; "bottom" to quantities associated with the bottom of the mixed layer; "below" to the water below the thermocline.

We adopt similar mixed boundary conditions on heat transfer at the upper and lower boundaries to relate heat flux to temperature differences across the interfaces. If T_a, T_s, T_{bottom}, and T_{below} are the temperatures of the air and water corresponding to U_a, u_s, u_{bottom}, and u_{below}, then Newton's law of cooling gives

$$\kappa_T\frac{\partial T}{\partial z} = h_{aw}(T_a - T_s) \quad \text{at} \quad z = 0, \qquad (5)$$

and

$$\kappa_T\frac{\partial T}{\partial z} = h_{ww}(T_{\text{bottom}} - T_{\text{below}}) \quad \text{at} \quad z = -d. \qquad (6)$$

Here h_{ww} is the heat transfer coefficient across the thermocline (heat flux divided by heat capacity, $\rho_w c_{pw}$, of a unit volume of water), h_{aw} is the heat flux across the air layer divided by the heat capacity of a unit volume of water, and κ_T is the (eddy) thermal diffusivity of water.

b. *Structureless equilibrium*

By a "structureless" state, we mean one depending only on depth and time. Horizontally averaged fields, for example, are by definition structureless. Our concern is with the stability and bifurcated states of time-independent structureless equilibria.

The CL theory differs from the Navier–Stokes or Reynolds-averaged Navier–Stokes equations by a term representing the rectified effects of surface gravity waves. These effects reside in a "vortex force"

$$\mathbb{U}_S \times \text{curl}\mathbf{v},$$

where $\mathbf{v}$ is the velocity vector of the complete (rectified) current system. When $\mathbb{U}_S = U_S(z)\mathbf{i}$, and the Coriolis acceleration is ignored, the CL equations allow for a nonconvective, rectilinear current and temperature field in which the vortex force does not play a role. When the Coriolis acceleration is accounted for, the vortex force is important in determining the structureless states in the mixed layer (see Huang 1979). While we recognize that the Coriolis acceleration generally may be expected to be nonnegligible in its effect on the structureless equilibria in the ocean, a satisfactory treatment of the combined "Langmuir–Ekman" layer is a complex matter. For the purposes of the present paper, which is to explore the effects of boundary conditions, we ignore the Coriolis acceleration.

Applications of the theory to date assume constant eddy viscosity and constant eddy thermal diffusivity. Although the theory is not restricted to this representation of the incoherent turbulence, we continue to adopt this parameterization.

Given these preliminary remarks, the problem for nonconvective or "structureless" states in the layer is (quasi)laminar and the vortex force term simply modifies the mean pressure distribution. If we seek steady

structureless equilibria, then the velocity vector lies in the horizontal plane and must be a linear function of z. Similarly, the temperature, $T(z)$, must be a linear function. The boundary conditions are (3), (4), (5), and (6).

Defining

$$R_* = \frac{u_* d}{\nu_T},$$

the velocity field satisfying the equations governing the CL theory, and the boundary conditions (3), (4), (5), and (6) has x component

$$u = U(z) = U_1 \frac{z}{d} + U_0, \tag{7}$$

where

$$U_0 = u_* \frac{(1 - m + \alpha_b)R_* + \alpha_b(u_{\text{below}}/u_*)}{\alpha_b + \alpha_t + \alpha_b\alpha_t} \tag{8}$$

and

$$U_1 = u_* \frac{(\alpha_b + m\alpha_t)R_* - \alpha_t\alpha_b(u_{\text{below}}/u_*)}{\alpha_b + \alpha_t + \alpha_b\alpha_t}, \tag{9}$$

where

$$\alpha_t = B_1 u_* R_* = \frac{2u_*}{U_a} R_* \quad \text{and} \quad \alpha_b = \frac{dw_e}{\nu_T} + C_{IW}R_* \tag{10}$$

are dimensionless parameters. In (10), B_1 has been replaced by the "simplistic" (and most likely extreme) choice. In accordance with the remarks following (3), α_t may be smaller, perhaps zero.

The y velocity component is

$$v = V(z) = \frac{\alpha_b v_{\text{below}}}{\alpha_t + \alpha_t\alpha_b + 2\alpha_b}\left(-\alpha_t \frac{z}{d} + 2\right). \tag{11}$$

In the work to follow, we assume that both α_t and α_b are nonnegative and that $(u_{\text{below}}, v_{\text{below}}) = \mathbf{0}$. (The latter assumption is always permissible, though not necessarily convenient, since we can always adopt a coordinate system moving with the fluid below at the expense of altering the specification of the wind and surface wave fields.)

The corresponding temperature field is given by

$$T(z) = T_1\left(\frac{z}{d} + l\right). \tag{12}$$

In (12),

$$T_1 \equiv \frac{T_a - T_{\text{below}}}{1 + \gamma_t^{-1} + \gamma_b^{-1}}, \tag{13}$$

and

$$l \equiv \frac{T_a + \gamma_b^{-1}T_a + \gamma_t^{-1}T_{\text{below}}}{T_a - T_{\text{below}}}, \tag{14}$$

where

$$\gamma_t = \frac{dh_{aw}}{\kappa_T}, \quad \text{and} \quad \gamma_b = \frac{dh_{ww}}{\kappa_T} \tag{15}$$

are Péclet numbers. The structureless temperature field may be statically stable or unstable. Density gradients are not necessary to the Langmuir circulation instability mechanism: the motions are not buoyancy driven. We shall think primarily of the situation in which the layer is stably stratified, but the case of unstable stratification is not excluded from the analysis we present.

c. *Typical parameter magnitudes*

We estimate the parameters α_t, α_b, γ_t, γ_b by parameterizing u_* and ν_T in terms of the wind speed, taking $u_*/U_a \sim 10^{-3}$, consistent with an air–sea momentum exchange coefficient $C_m = \mathrm{O}(10^{-3})$, as is generally reported [e.g., see Busch (1977) for typical values]. This implies the (extreme) estimate

$$\alpha_t \sim 2 \times 10^{-3} R_*.$$

The question of the loss of momentum from the mixed layer to internal waves is too difficult for us to address here. In many cases, we expect that this momentum transfer will be small compared to the direct loss to entrainment [see the discussions of this point by Niiler and Kraus (1977) and by Kantha (1977)]. In any event, for the present purposes, we take $C_{IW} = 0$ in estimating the parameter α_b.

According to the experiments of Kantha and Phillips (1976) in a two-layer stratified water body driven by an applied surface stress, the light turbulent upper layer entrains nonturbulent heavy fluid with an entrainment velocity given by

$$w_e = u_* f(\mathrm{Ri}).$$

Here the overall Richardson number is

$$\mathrm{Ri} = \frac{gd}{u_*^2}\frac{\Delta\rho}{\rho};$$

$\Delta\rho$ is the difference in density between the heavy and light fluid, and f is a function that at present must be experimentally determined. The data from the Kantha/Phillips experiment, as discussed by Phillips (1977), suggest the rough approximation to this function:

$$\frac{w_e}{u_*} \sim \frac{6}{\mathrm{Ri}}. \tag{16}$$

If (16) is used to estimate the entrainment velocity in α_b,

$$\alpha_b \sim \frac{6}{\mathrm{Ri}} R_*.$$

Relating the friction velocity to the wind speed shows that

$$\mathrm{Ri} = \left(\frac{U_a}{u_*}\right)^2 \frac{gd}{U_a^2}\frac{\Delta\rho}{\rho} \sim 10^6 \frac{gd}{U_a^2}\frac{\Delta\rho}{\rho}.$$

For purposes of estimating, we will take $\Delta\rho/\rho \sim 10^{-3}$ as a plausible value for the fractional density "jump" across the pycnocline terminating the mixed layer, then

$$\alpha_b \sim 6 \times 10^{-3} \frac{U_a^2}{gd}\frac{u_* d}{\nu_T}.$$

From this, we arrive at the estimate $\alpha_t/\alpha_b \sim (1/3)gd/U_a^2$. For a wind speed of 25 m s^{-1} and a mixed-layer depth of 50 m, the ratio is about 0.26. For a wind speed of 10 m s^{-1}, and the same depth, the ratio is about 1.5.

Returning now to the estimation of α_t, we assume a parameterization of ν_T similar to that quoted in Leibovich and Radhakrishnan (1977), $\nu_T \sim 2.5 \times 10^{-5} U_a^3/g$. Then,

$$\alpha_t \sim 10^5 \times \left(\frac{u_*}{U_a}\right)^2 \frac{gd}{U_a^2}.$$

Again assuming $u_*/U_a = 10^{-3}$, a mixed-layer depth of 50 m and a 25 m s^{-1} wind, we get $\alpha_t \approx 0.06$. Choosing the eddy viscosity to be proportional to U_a^3/g, as we have done here, makes α_b independent of the wind speed and mixed-layer depth. With the specific parameterization introduced above, $\alpha_b \sim 0.24$.

By comparing with the data on the transfer of sensible heat at the air–sea interface given by Busch (1977), we find our exchange coefficient to be

$$h_{aw} = \frac{[\rho c_p]_{\mathrm{air}}}{[\rho c_p]_{\mathrm{water}}} U_a C_\theta,$$

where the conventional bulk exchange coefficient for heat, C_θ, is approximately the same as C_m. Our dimensionless heat exchange coefficient at the surface is

$$\gamma_t \sim \frac{3C_\theta \times 10^{-4}}{(u_*/U_a)}\frac{u_* d}{\kappa_T}. \tag{17}$$

This shows that

$$\gamma_t \sim \frac{0.15\alpha_t}{\tau}, \quad \text{where} \quad \tau \equiv \frac{\kappa_T}{\nu_T}.$$

The parameter τ is an inverse Prandtl number. The molecular value of τ is about 0.15, but a more likely value when based on turbulent diffusivities of heat and momentum would probably be around unity. In either event, when α_t is small, so is γ_t.

At the base of the mixed layer, it seems reasonable to set $h_{ww} = w_e$, then

$$\gamma_b = \frac{w_e d}{\kappa_T} = \frac{\alpha_b}{\tau}, \tag{18}$$

so γ_b is comparable to α_b.

The arguments in this section suggest that for mixed-layer depths not much larger than 50 m and for high wind speeds, $\alpha_t \ll \alpha_b$, so that the correction to the constant stress model is more important at the base of the mixed layer. Since we expect α_t to be less than the extreme expression used for the above estimates, we are inclined to think that the constant stress model is adequate at the air–sea interface. Nevertheless, α_t will be carried through the analysis that follows.

3. The governing equations for dimensionless quantities

We now set up the dimensionless problem to be satisfied by the perturbations to the basic state [(7), (12)]. From here on, a superscript asterisk denotes a dimensional quantity. We assume that variations in the x^* direction are negligible, so the motions are two dimensional. A streamfunction, ψ^*, may then be used in lieu of the velocity components v^* and w^* in the y^* and z^* directions. We make the problem dimensionless as follows:

$$y = y^*/d, \quad z = z^*/d, \quad t = t^*\nu_T/d^2,$$
$$u = (u^* - U(z))/U_1, \quad \psi = \psi^*/\nu_T,$$
$$v = \frac{\partial\psi}{\partial z} = v^* d/\nu_T, \quad w = -\frac{\partial\psi}{\partial y} = w^* d/\nu_T,$$
$$\theta = (\theta^* - T(z))/T_1,$$

where ψ, u, and θ are the streamfunction, the perturbation to the velocity component in the wind direction, and the temperature perturbation, respectively. Substituting these expressions into the governing wave-filtered Navier–Stokes and heat equations, we find the governing equations for ψ, u, and θ to be (Leibovich 1985; Leibovich et al. 1989)

$$\left(\frac{\partial}{\partial t} - \nabla^2\right)\nabla^2\psi = Rh(z)\frac{\partial u}{\partial y} - S\frac{\partial\theta}{\partial y} + J(\psi, \nabla^2\psi),$$
$$\left(\frac{\partial}{\partial t} - \nabla^2\right)u = \frac{\partial\psi}{\partial y} + J(\psi, u),$$
$$\left(\frac{\partial}{\partial t} - \tau\nabla^2\right)\theta = \frac{\partial\psi}{\partial y} + J(\psi, \theta). \tag{19}$$

The parameters in these equations are

$$R = \frac{U_1 d^3}{\nu_T^2}\frac{\partial U_S^*}{\partial z}(0), \quad S = \frac{\beta g T_1 d^3}{\nu_T^2}, \tag{20}$$

which represent the destabilizing vortex force and the stratification, respectively, where β is the coefficient of thermal expansion, and g is the acceleration due to gravity. The function $h(z)$ is the dimensionless Stokes-drift gradient, so

$$\frac{\partial U_S^*}{\partial z}(z) = \frac{\partial U_S^*}{\partial z}(0)h(z),$$

where $U_S^*(z)$ is the Stokes drift (in the x^* direction). The Jacobian is defined by $J(a, b) = a_y b_z - a_z b_y$.

The dimensionless versions of the boundary conditions on the perturbation velocity field, using the stress model introduced in (3) and (4) are

$$\frac{\partial^2 \psi}{\partial z^2} + \frac{1}{2}\alpha_t \frac{\partial \psi}{\partial z} = \frac{\partial u}{\partial z} + \alpha_t u = 0 \quad \text{on} \quad z = 0, \quad (21)$$

and

$$\frac{\partial^2 \psi}{\partial z^2} - \alpha_b \frac{\partial \psi}{\partial z} = \frac{\partial u}{\partial z} - \alpha_b u = 0 \quad \text{on} \quad z = -1. \quad (22)$$

The corresponding conditions on the dimensionless perturbation temperature are

$$\frac{\partial \theta}{\partial z} + \gamma_t \theta = 0 \quad \text{on} \quad z = 0, \quad (23)$$

and

$$\frac{\partial \theta}{\partial z} - \gamma_b \theta = 0 \quad \text{on} \quad z = -1. \quad (24)$$

The remaining boundary conditions on ψ are that the vertical velocity vanishes on the planes $z = 0, -1$, so

$$\psi = 0 \quad \text{on} \quad z = 0, -1. \quad (25)$$

We analyze the linear stability of the basic state [(7), (12)] by dropping the nonlinear Jacobian terms from (19) and considering disturbances that are normal modes proportional to $e^{iky+\sigma t}$, where k is the horizontal wavenumber and σ is the linear growth rate. For sufficiently small values of R, all modes are damped [$\mathrm{Re}(\sigma) < 0$], and so the basic state is stable to small disturbances. As R is increased through a threshold critical value, R_c, the basic state is destabilized. This occurs when the real part of the growth rate of some mode, whose wavenumber we denote by k_c, becomes positive.

When α_t and α_b both vanish (so the perturbation stress vanishes on the boundaries), the critical wavenumber, k_c, is zero, so the first motions to become linearly unstable occur on the largest horizontal scale available. This consequence of these (or mathematically analogous) boundary conditions is seen in a variety of other convective systems, for example in Rayleigh–Bénard convection between nonconducting surfaces (Sparrow et al. 1964; Nield 1967; Chapman and Proctor 1980; Chapman et al. 1980; Gertsberg and Sivashinsky 1981; Depassier and Spiegel 1982), which is mathematically identical to the two-dimensional CL theory without thermal stratification; in surface tension–driven (Marangoni) convection (Sivashinsky 1982); in the directional solidification of a dilute binary alloy (Sivashinsky 1983); in mildly penetrative ice–water convection (Roberts 1985). In all these examples, a shallow water approximation that exploits the disparity between horizontal and vertical length scales allows one to derive a model equation that describes the nonlinear evolution of the long-wavelength disturbances.

When the α are nonzero (from their definitions, they are always nonnegative), a finite horizontal length scale of the convective motions at onset is found. For typical conditions, the estimates of section 2 indicate that the α are small, and below we calculate the linear growth rate of Langmuir circulations under this assumption. Figure 2 illustrates the qualitative difference between the marginal stability curves for $\alpha_t + \alpha_b = 0$ and $\alpha_t + \alpha_b \neq 0$: in the former case, the first motions to become unstable as R is increased have infinite wavelength (equivalently, $k_c = 0$), while in the latter their wavelength is finite ($k_c > 0$).

4. Calculation of the growth rate, σ

a. Analysis of small-k disturbances

When $\alpha \equiv \alpha_t + \alpha_b$ is small, the critical wavenumber is small also, $k_c = O(\alpha^{1/4})$ (see Proctor 1981; Gertsberg and Sivashinsky 1981). In this section we give the first few terms in a small-k expansion for the linear growth rate of small disturbances. The details of the calculations are given in the Appendix. There are two cases, $\gamma \equiv \gamma_t + \gamma_b > 0$ and $\gamma = 0$, which must be treated separately. Since the physical problem suggests examination of small γ, we follow the two analyses with a discussion on the crossover between the two cases. We treat in detail only the case of constant Stokes drift gradient, $h(z) = 1$, which is the most analytically tractable, and describe results for more general expressions for $h(z)$ in a later section.

We expand the variables in powers of k,

$$\begin{aligned} \psi &= i(k\psi_1 + k^3\psi_3 + \cdots)e^{iky}e^{\sigma t}, \\ u &= (u_0 + k^2u_2 + k^4u_4 + \cdots)e^{iky}e^{\sigma t}, \\ \theta &= (\theta_0 + k^2\theta_2 + k^4\theta_4 + \cdots)e^{iky}e^{\sigma t}, \\ \sigma &= k^2\sigma_2 + k^4\sigma_4 + \cdots, \\ R &= R_0 + k^2R_2, \end{aligned} \quad (26)$$

where each of the coefficients, ψ_j, u_j, θ_j is a function of z alone. The expressions in (26) are substituted into the governing linearized equations, which are then solved at successive orders in k. It turns out that the appropriate scaling for small α is $k = O(\alpha^{1/4})$, so we write $(\alpha_t, \alpha_b) = k^4(\bar{\alpha}_t, \bar{\alpha}_b)$, where $\bar{\alpha}_{t,b} = O(1)$. Similarly we define $\bar{\alpha} = \bar{\alpha}_t + \bar{\alpha}_b$.

At $O(k^0)$ in the governing equations,

$$D^2u_0 = 0 \quad \text{and} \quad D^2\theta_0 = 0, \quad (27)$$

where $D \equiv d/dz$. To this order, the boundary conditions are that $Du_0 = 0$ on $z = 0, -1$, and that $D\theta_0 = -\gamma_t\theta_0$ on $z = 0$, and $D\theta_0 = \gamma_b\theta_0$ on $z = -1$. Therefore, u_0 is a constant, and we see that there are two cases for

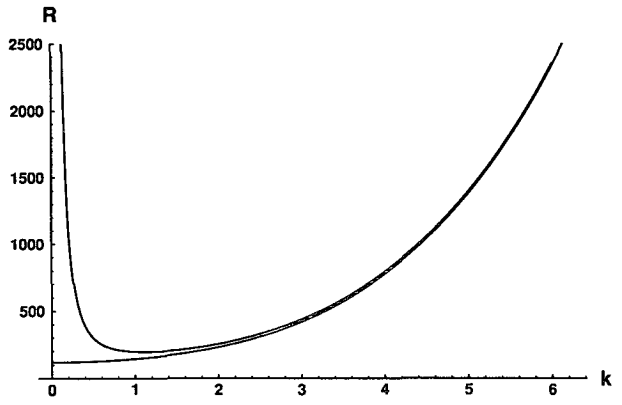

FIG. 2. Critical Rayleigh number, R_c, for the onset of convection plotted against the wavenumber, k. The fluid is unstratified ($S = 0$), and the parameters R and S are as given by (20). For the lower curve, the parameters α_b and α_t are both zero and as a result, the critical wavenumber is $k_c = 0$. Here the widest rolls are the first to be destabilized. For the upper curve α_b and α_t take the values 0.28 and 0.06, respectively, which are typical magnitudes of these parameters in the ocean. Now the widest rolls are stabilized, and at onset the motions have a finite wavelength ($k_c \approx 1.1$).

θ_0. If $\gamma > 0$, then $\theta_0 = 0$, but if $\gamma = 0$, then θ_0 is an arbitrary constant.

b. Growth rate of small-k disturbances when $\gamma > 0$: Case I

We consider now the first case (which we call "I"), where $\gamma > 0$. The algebra is described in the Appendix and yields the following expression for the growth rate σ for small-wavenumber disturbances:

$$\sigma = -\alpha + \frac{R - R_0}{R_0} k^2 - \left(\frac{1091}{5544} + \Sigma \frac{691\gamma_t\gamma_b + 2077\gamma + 5544}{5544(\gamma_t\gamma_b + \gamma)}\right)k^4 + O(k^6). \quad (28)$$

The parameter $S/(120\tau)$ occurs frequently in what follows, so we have represented it by the symbol Σ in (28) and in expressions that will follow. We have also replaced the sum $\gamma_t + \gamma_b$ by the symbol γ. Lele (1985) has calculated this expression for σ in the special case $\alpha_{t,b} = \gamma_{t,b}^{-1} = 0$, but his expression for the coefficient of k^4 contains an error.

c. Growth rate of small-k disturbances when $\gamma = 0$: Case II

We now turn to case II, where $\gamma = 0$, so that at leading order there is a nontrivial solution to (27) where both u_0 and θ_0 are nonzero constants. Then,

$$D^4\psi_1 = -R_0u_0 + S\theta_0,$$

subject to the boundary conditions $D^2\psi_1 = \psi_1 = 0$ on $z = 0, -1$, which has the solution

$$\psi_1 = -(R_0u_0 - S\theta_0)(z^4/24 + z^3/12 - z/24).$$

At $O(k^2)$ we find

$$\sigma_2u_0 - D^2u_2 = -u_0 - \psi_1, \quad (29)$$

$$\sigma_2\theta_0 - \tau D^2\theta_2 = -\tau\theta_0 - \psi_1. \quad (30)$$

Integrating both of these equations across the layer, we find

$$\begin{pmatrix} \sigma_2 + 1 - R_0/120 & S/120 \\ -R_0/120 & \sigma_2 + \tau + S/120 \end{pmatrix}\begin{pmatrix} u_0 \\ \theta_0 \end{pmatrix} = \begin{pmatrix} 0 \\ 0 \end{pmatrix}, \quad (31)$$

and for a nontrivial leading-order solution the determinant of the matrix must vanish; that is,

$$120\sigma_2^2 + (S + 120\tau + 120 - R_0)\sigma_2 + (S + 120\tau - \tau R_0) = 0. \quad (32)$$

We now determine the values of R_0 at which the basic state becomes unstable to steady or oscillatory convection. The onset of steady convection occurs when one root of the quadratic (32) passes through zero, while the other is negative. One root is zero when $R_0 = R_S$, where

$$R_S = 120(1 + \Sigma).$$

At this point the second root is

$$\sigma_2 = \Sigma(1 - \tau) - \tau,$$

which is negative provided

$$(1 - \tau)\Sigma < \tau.$$

Alternatively, the basic state becomes unstable to oscillatory convection when the roots of the quadratic (32) are $\sigma_2 = \pm i\omega$ (with ω real), at $R_0 = R_H$, say. We find that

$$R_H = 120[1 + \tau(1 + \Sigma)]$$

and that

$$\omega^2 = \tau[(1 - \tau)\Sigma - \tau].$$

This bifurcation can, therefore, occur only when

$$(1 - \tau)\Sigma > \tau.$$

We note that whenever this condition is fulfilled $R_H - R_S = -120\omega^2/\tau < 0$, so the oscillatory bifurcation is the first bifurcation of the basic state as R is increased.

When $\gamma = 0$, then, there are two subcases according to the sign of $(1 - \tau)\Sigma - \tau$. We consider first the case ["II(S)"], where this quantity is negative, so the basic state becomes unstable to steady convection, that is, $\sigma_2 = 0$ when $R_0 = R_S$. The solvability condition (31) then requires that $\theta_0 = u_0/\tau$, and with no loss of generality we take $u_0 = 1$. The remaining algebra necessary

for the derivation of the growth rate is given in the Appendix and yields

$$\left(1 + \frac{\Sigma(\tau - 1)}{\tau}\right)\sigma = -\alpha(1 + \Sigma) + \frac{R - R_S}{120}k^2 - \frac{1091}{5544}k^4 + O(k^6). \quad (33)$$

In case II(H), when $(1 - \tau)\Sigma - \tau > 0$, the growth rate has a nonzero imaginary part, $\sigma_i = \pm i\omega k^2 + O(k^4)$, and so the convection is oscillatory. The expressions for the real and imaginary parts of the growth rate are rather messy and are given in the Appendix.

d. *Analysis of the expressions for the growth rate*

In all cases, the real part of the growth rate [given by (28), (33), or (55)] is of the form

$$\mathrm{Re}(\sigma) = -c_1\alpha + (R - R_0)k^2/c_2 - c_3k^4 + O(k^6), \quad (34)$$

where the coefficients are summarized in Table 1. To this order in the calculation, α_t and α_b occur in the expression for the growth rate only in the combination $\alpha = \alpha_t + \alpha_b$; they occur independently at higher order in the expansion for σ.

For a given value of R, the largest growth rate occurs for the mode with wavenumber $k_{\max} = [(R - R_0)/(2c_2c_3)]^{1/2}$. This wavenumber is independent of α: even for the CSM, with $\alpha = 0$, the fastest-growing mode has a finite wavelength whenever $R > R_0$. It is the *nonlinear* cascade to the widest cells that results in the Langmuir circulations of the CSM taking the largest horizontal length scale available [see Chapman and Proctor (1980), for the analogous cascade in Rayleigh–Bénard convection]. Such a cascade is possible in the CSM because the largest scales are the first to become unstable and are unstable whenever $R > R_0$. We can immediately identify in (34) the role of $\alpha > 0$ in stabilizing these modes, because $\mathrm{Re}(\sigma) \to -c_1\alpha < 0$ as $k \to 0$. We, therefore, expect that the cascade to the largest possible scales does not occur when $\alpha > 0$, because the widest cells are stable.

Instability occurs first when $R = R_c$ and $k = k_c$, where

$$R_c = R_0 + 2c_2(c_1c_3\alpha)^{1/2}, \quad k_c = (c_1\alpha/c_3)^{1/4}. \quad (35)$$

Thus, for small $\alpha > 0$ the critical wavenumber grows rapidly with α (Proctor 1981; Gertsberg and Sivashinsky 1981; Sivashinsky 1982, 1983).

c. *The competition between cases I and II when* $\Sigma \neq 0$

When $\Sigma = 0$, cases I and II above collapse to case I. The temperature of the water column is uniform, and the value of γ therefore is irrelevant. On the other hand, when $\Sigma \neq 0$, we have arrived at results that can be qualitatively different depending on whether γ is zero or nonzero. In the first instance, we of course do not mean that γ is really zero, but that it is small compared to α. In application to physical problems, it may be unclear which expression for the growth rate [that is, (28), (33), or (55)] is appropriate for given values of the parameters. This question, whether instability I or II occurs first as R is increased, can ultimately be resolved only by solving numerically the full linear stability problem obtained from (19) and (21)–(25). In the small-wavenumber limit that arises in practice, however, we can provide an asymptotic estimate of when each case applies, for the (physically realistic) limit as $\gamma \to 0$. We assume throughout this section that α is small, and our remarks are specifically in the context of the small-wavenumber theory developed in this paper. If the critical wavenumber of the full numerical linear stability problem is too large then the expansion (26) we have considered becomes invalid, and the full numerical solution must be used.

Figure 3 illustrates the competition between instability according to case I and instability according to case II(H). Several marginal stability curves are plotted on this figure, for various values of γ, with all the other parameters fixed. The lowest curves on the figure are those for the largest values of γ and correspond to steady convection (case I). As γ is decreased, the steady marginal curve is restricted to smaller values of k, and the critical Rayleigh number, R_c, for steady convection

TABLE 1. Coefficients of the expression (34) for the growth rate σ in the three cases: I, $\gamma > 0$, steady convection; II(S), $\gamma = 0$, steady convection; II(H), $\gamma = 0$, oscillatory convection.

	c_1	c_2	$5544c_3$	R_0
I	1	120	$\dfrac{1091 + 691\Sigma + 1386\Sigma}{\gamma + \gamma_t\gamma_b}$	120
II(S)	$\dfrac{1 + \Sigma}{1 + \Sigma(\tau - 1)/\tau}$	$120\left(1 + \dfrac{\Sigma(\tau - 1)}{\tau}\right)$	$\dfrac{1091}{1 + \Sigma(\tau - 1)/\tau}$	$120(1 + \Sigma)$
II(H)	$\dfrac{1}{2}$	240	$\dfrac{1}{2}[\Sigma(1 - \tau)(31 - 530\tau) + (\tau + 1)(530\tau + 1091)]$	$120[1 + \tau(1 + \Sigma)]$

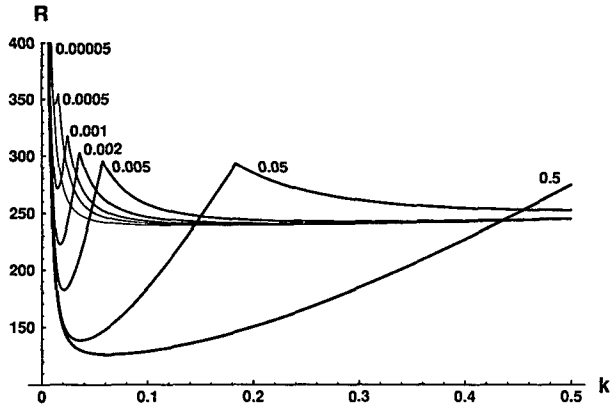

FIG. 3. Critical Rayleigh number, R_c, plotted against the wavenumber, k, for stratification $S = 100$ and inverse Prandtl number $\tau = 1/6.7$. The parameters R and S are given by (20). The curves are all for $\alpha_t = \alpha_b = 0.5 \times 10^{-4}$, and in increasing order of line thickness correspond to $\gamma_t = \gamma_b = 0.5 \times 10^{-4}$, 0.5×10^{-3}, 1.0×10^{-3}, 2.0×10^{-3}, 0.5×10^{-2}, 0.5×10^{-1}, 0.5. The flat parts of the curves to the right of the diagram represent the stability margin for oscillatory convection [case II(H)]; the approximately parabolic parts of the curves to the left of the diagram represent the stability margin to steady convection (case I). For the smaller values of γ, the first bifurcation is oscillatory, and the appropriate analysis is that which assumes $\gamma = 0$ [case II(H)]; the larger values of γ give a steady onset of convection, and the appropriate case is I. The crossover between steady and oscillatory convection is seen to occur for a value of γ between 2.0×10^{-3} and 4.0×10^{-3}. The value of α was chosen artificially small in order to illustrate clearly the competition between the two modes of instability.

increases. Eventually, the first instability is no longer to the steady mode, but to the oscillatory mode, II(H). We now analyze this competition and the similar competition that arises between instabilities I and II(S) for smaller values of the stratification parameter, S, and we compute criteria for deciding which mode is destabilized first.

First, we note that if we set $\gamma = 0$ in the model, the instability is always case II. We then consider the quantity $Q = (1 - \tau)\Sigma - \tau$. If $Q < 0$ then the bifurcation of the structureless equilibrium is to steady convection, and we take case II(S); if the inequality is reversed, then oscillatory convection occurs, and so we take case II(H).

When $\gamma > 0$, however, there are two modes that compete for the first instability of the basic state. If $Q < 0$ these are modes I and II(S), while if $Q > 0$ they are I and II(H). For arbitrary $\gamma > 0$ the appropriate growth rate in the limit as $k \to 0$ is that of case I, for steady convection. (This is shown in Fig. 3, for the leftmost part of each marginal curve.) Therefore, whatever the value of γ, provided it is larger than zero, there is a steady bifurcation for sufficiently small k. The important issue is which instability occurs at the critical wavenumber, k_c. We now estimate this for the case of small (but positive) γ, where there is competition between I and either II(S) or II(H) (according to the sign of Q). To decide between I and II, we note first that in the limit as $\gamma \to 0$, the critical Rayleigh numbers of the three cases are, from (35),

$$R_c(\mathrm{I}) \sim 120\left(1 + 2\left\{\frac{\alpha\Sigma}{\gamma}\right\}^{1/2}\right)$$

$$R_c(\mathrm{II(S)}) \sim 120\left(1 + \Sigma + 2\left\{\alpha(1 + \Sigma)\frac{1091}{5544}\right\}^{1/2}\right)$$

$$R_c(\mathrm{II(H)}) \sim 120(1 + \tau(1 + \Sigma) + (8\alpha c_3)^{1/2}).$$

These expressions are correct to leading order in Σ/γ, as are the following computations. There are two cases.

First, if $Q < 0$ then we observe that $R_c(\mathrm{II(S)}) - R_c(\mathrm{I})$ has the same sign as $\gamma - \gamma_S$, where

$$\gamma_S = \frac{4\alpha}{\Sigma}.$$

We are concerned with the first instability of the basic state as R is increased, so case I applies whenever $\gamma > \gamma_S$, and case II(S) whenever this inequality is reversed. In the second case, $Q > 0$, we note that $R_c(\mathrm{II(H)}) - R_c(\mathrm{I})$ has the same sign as $\gamma - \gamma_H$, where

$$\gamma_H = \frac{4\Sigma\alpha}{(1 + \Sigma)^2\tau^2}. \tag{36}$$

The critical wavenumber corresponds to steady convection of case I if $\gamma > \gamma_H$ and oscillatory convection if the inequality is reversed. The crossover between steady instability (I) and oscillatory instability [II(H)] in Fig. 3 occurs for a value of γ between 2.0×10^{-3} and 4.0×10^{-3}. This is consistent with the estimate (36), which gives for those parameter values $\gamma_H \approx 2.3 \times 10^{-3}$. (We have used an artificially small value of α in this example.)

We emphasize that these expressions are formally valid in the limit as $\gamma \to 0$ [and the selection of II(S) or II(H) according to the sign of Q is based on an analysis of the problem when $\gamma = 0$], so that the dividing lines between the cases given here are approximate. Clearly these guidelines on the choice of cases fail if γ_S or γ_H (as appropriate) is not small.

5. Nonlinear evolution

The disparity between the horizontal and vertical length scales of the motions when α_t and α_b are small may be exploited for the derivation of a *nonlinear* evolution equation for the Langmuir circulations [see Chapman and Proctor (1980) for the Rayleigh–Bénard problem between fixed-flux boundaries]. We emphasize, as do Chapman and Proctor (1980), that this evolution equation results not from a small-amplitude expansion, but from a long-wavelength approximation and, therefore, its solutions are not restricted to be of small amplitude. In fact u may be $O(1)$, while $v = O(u_y)$ and $w = O(u_{yy})$, where for the nonlinear problem $\partial/\partial y$ replaces the wavenumber as the small expansion parameter.

The derivation of the nonlinear equation for Langmuir circulations is similar to the derivation above of the small-k expansion for σ but the nonlinear terms are retained.

For constant Stokes drift gradient, $h(z) = 1$, it is feasible to compute the coefficients exactly. For case I, that is, for $\gamma > 0$, the equation is

$$\frac{\partial u}{\partial t} = -\alpha u - \frac{R - R_0}{R_0}\frac{\partial^2 u}{\partial y^2} - \left(\frac{1091}{5544} + \Sigma\frac{691\gamma_t\gamma_b + 2077\gamma + 5544}{5544(\gamma_t\gamma_b + \gamma)}\right)\frac{\partial^4 u}{\partial y^4} + \frac{155}{126}\frac{\partial}{\partial y}\left(\frac{\partial u}{\partial y}\right)^3, \quad (37)$$

where $R_0 = 120$,

$$\psi = u_y P(z) + O(u_{yyy}), \quad (38)$$

with

$$P(z) = -5z^4 - 10z^3 + 5z, \quad (39)$$

and

$$\theta = u_{yy}Q(z) + O(u_{yyyy}), \quad (40)$$

with

$$Q(z) = \left(\frac{z^6}{6} + \frac{z^5}{2} - \frac{5z^3}{6} + \frac{(\gamma_b + 2)(\gamma_t z - 1)}{2(\gamma_t\gamma_b + \gamma)}\right)\Big/\tau. \quad (41)$$

In case II(S), the steady convection that occurs when $\gamma = 0$ and $(1 - \tau)\Sigma < \tau$ is governed by

$$\left(1 + \frac{\Sigma(\tau - 1)}{\tau}\right)\frac{\partial u}{\partial t} = -\alpha(1 + \Sigma)u - \frac{R - R_S}{120}\frac{\partial^2 u}{\partial y^2} - \frac{1091}{5544}\frac{\partial^4 u}{\partial y^4} + \frac{155}{126}\left(1 + \frac{\Sigma(\tau^2 - 1)}{\tau^2}\right)\frac{\partial}{\partial y}\left(\frac{\partial u}{\partial y}\right)^3, \quad (42)$$

where ψ is given by (38), but now $\tau\theta = u + O(u_{yy})$.

a. *Nonconstant Stokes-drift gradient*

For a monochromatic wave train the Stokes-drift gradient takes the form $h(z) = e^{2\kappa z}$, where κ is proportional to the wavenumber of the surface waves. In the above analysis for constant $h(z)$ we have taken the limiting case $\kappa = 0$. We have generalized our results to other values of κ, but in practice we find that we must perform these computations numerically because the algebra involved in using the exact expressions is prohibitive. As an example we treat the case $\gamma > 0$, in fact the extreme case $\gamma_t = \gamma_b = \infty$, so the thermal boundary conditions are that $\theta = 0$ at $z = 0, -1$.

Equation (37) is invariant under the mapping $u \to -u$, which follows from the up–down symmetry of the problem when $\kappa = 0$. (When $\alpha_t \neq \alpha_b$ or $\gamma_t \neq \gamma_b$ this symmetry is weakly broken.) If, however, the Stokes-drift gradient is not constant then the up–down symmetry of the problem is broken, and a symmetry-breaking term appears on the right-hand side of (37). The evolution equation for u then takes the form

$$\frac{\partial u}{\partial t} = -\alpha u - \frac{R - R_0}{R_0}\frac{\partial^2 u}{\partial y^2} - (a_1 + a_2\Sigma)\frac{\partial^4 u}{\partial y^4} + b\frac{\partial}{\partial y}\left(\frac{\partial u}{\partial y}\right)^3 + d\frac{\partial^2}{\partial y^2}\left(\frac{\partial u}{\partial y}\right)^2. \quad (43)$$

Note that the parameters α_t and α_b occur in (43) only as the sum $\alpha = \alpha_t + \alpha_b$. This is just as we noted for the case $\kappa = 0$ in section 4d: the up–down asymmetry of the problem when $\kappa \neq 0$ does not change the equal mathematical role of the α's (to leading order). The critical value R_0 has been calculated by Lele (1985) for general values of κ and is

$$R_0 = 32\kappa^5/[1 - \kappa + \kappa^3/3 - e^{-2\kappa}(1 + \kappa - \kappa^3/3)].$$

Lele has pointed out that $R_0 \sim 96\kappa^2$ as $\kappa \to \infty$, in which limit the scaling that we have used for the layer depth becomes inappropriate, and a more appropriate scaling would be based instead on the depth of influence of the Stokes drift.

In Table 2 we give the coefficients of (43) for various values of the Stokes-drift parameter, κ, when $\gamma_t = \gamma_b = \infty$. Coefficients a_1, a_2, and b are only weakly dependent on κ, and the only coefficient that varies significantly is d, which multiplies the symmetry-breaking term $(u_y^2)_{yy}$.

By rescaling y, t, and u we find that equations of the form (43) have only two independent parameters, one that quantifies the instability (and which depends on $\alpha_{t,b}$, $\gamma_{t,b}$, R–R_0, and κ), and one that quantifies the departure from up–down symmetry (and which depends only on κ and $\gamma_{t,b}$). For a given initial-value problem, however, a third parameter will be the length of the computational domain. Numerical investigations by Chapman and Proctor (1980) and Chapman et al.

TABLE 2. Coefficients of the evolution equation (43) for various values of the Stokes-drift parameter, κ. The limiting values of the coefficients a_1, a_2, b, d as $\kappa \to \infty$ are, respectively, 1/5, 31/252, 128/105, 99/140. Note that, apart from d, the coefficients are only weakly dependent on κ.

κ	a_1	a_2	b	d
0	0.197	0.125	1.230	0
1.0	0.197	0.124	1.230	0.158
2.0	0.196	0.124	1.230	0.295
5.0	0.196	0.124	1.227	0.530
10.0	0.198	0.123	1.223	0.644
100.0	0.200	0.123	1.219	0.706
∞	0.2	0.123	1.219	0.707

(1980) for the case $\alpha = 0$ indicated that the convection took the largest horizontal scale available to it. Some particular numerical simulations by Sivashinsky (1982) and Gertsberg and Sivashinsky (1981) with $\alpha > 0$ showed that for mild supercriticality the nonlinear solutions of (43) equilibrate to convection cells of finite width, whose wavelength is close to the wavelength of maximum linear growth. We therefore expect that for $\alpha > 0$ a similar result will hold for Langmuir circulations, and that they will develop a finite wavelength.

6. Discussion

The form of the convective motion for γ fixed, and nonzero in the limit as $\alpha \to 0$, that is, in case I, may be inferred from (38) and (40). To lowest order,

$$\psi = u_y P(z), \quad \theta = u_{yy} Q(z), \tag{44}$$

where P and Q are the polynomials given in (39) and (41) if $\kappa = 0$ and are transcendental functions of z for all other choices of Stokes drift. Consequently, the horizontal and vertical velocity components are given by, respectively,

$$v = u_y P'(z), \quad w = -u_{yy} P(z), \tag{45}$$

and the horizontally averaged convective heat flux across any horizontal plane is

$$-\overline{w\theta} = \overline{u_{yy}^2} H(z), \tag{46}$$

where $H(z) = P(z)Q(z)$, and the overbar indicates the horizontal average.

In Fig. 4 we show the depth dependence of $P(z)$ in two cases: $\kappa = 0$ and $\kappa = \infty$. In the first case the polynomial is symmetrical about the midline $z = -1/2$; in the second, for which we find $P(z) = 8z + 12z^2 + 4z^3$, this symmetry is lost, reflecting the asymmetry of the Stokes-drift gradient. Contour plots of the streamfunction are given in Fig. 5 for the same values of κ. We have chosen an aspect ratio of π for the Langmuir circulation cells, which corresponds to a typical value of $k_c \approx 1$. For $\kappa = 0$ the motions are symmetrical about $z = -1/2$, while for $\kappa = \infty$ the Stokes-drift gradient is confined to a thin layer near the surface, and the convective motions are strongest there. Note that, according to (39) and (41), $P(z) < 0$ and $Q(z) < 0$ in the layer. From (45), the sweeping (v) component of the velocity vanishes where the windward velocity component u is either a maximum or a minimum. Furthermore, when u is a maximum, $u_{yy} < 0$, so downwelling occurs below lines of surface convergence, and these correspond to locations of maximum windward current. At the same location, $\theta > 0$, corresponding to a surface temperature excess. Similarly, upwelling, temperature deficits, and minima of the windward current coincide. These features are familiar in Langmuir circulations and follow from simple physical considerations.

The heat flux from the air to the sea surface is

$$k \frac{T_1}{d} [1 - \gamma_t \theta(y, 0, t)], \tag{47}$$

and the heat flux from the mixed layer to the water below is

$$k \frac{T_1}{d} [1 + \gamma_b \theta(y, -1, t)]. \tag{48}$$

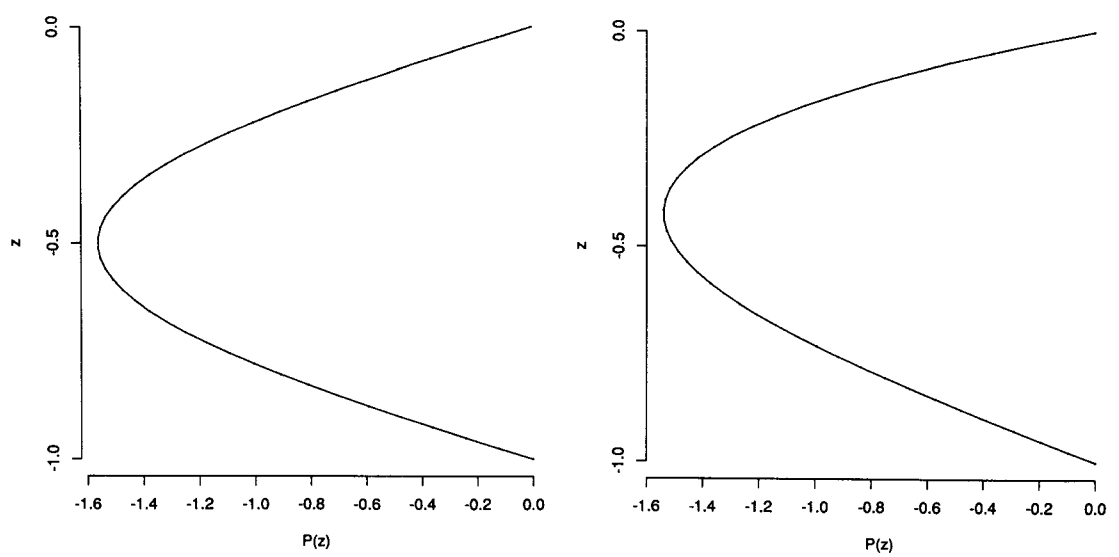

FIG. 4. Plots of $P(z)$ against z, where the streamfunction is $\psi = u_y P(z)$ [see (44)].
(i) $\kappa = 0$: $P(z) = -5z^4 - 10z^3 + 5z$; (ii) $\kappa = \infty$: $P(z) = 4z^3 + 12z^2 + 8z$.

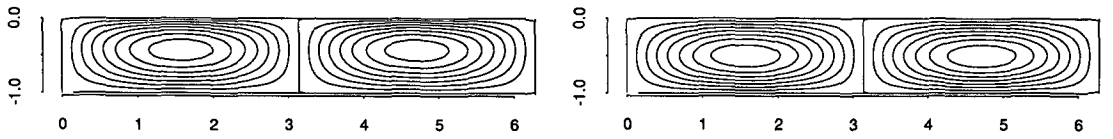

FIG. 5. Contour plots of the streamfunction ψ determined from linear theory, $\psi = P(z)\sin ky$. We have chosen the wavenumber to be $k = 1$, a value typical of those predicted by our theory. The width of each Langmuir circulation cell is then π times its depth. There is upwelling at $y = 0, 2\pi$ and downwelling at $y = \pi$, each of equal magnitude according to the linear theory. (i) $\kappa = 0$: $P(z) = -5z^4 - 10z^3 + 5z$; (ii) $\kappa = \infty$: $P(z) = 4z^3 + 12z^2 + 8z$.

The net heat flux, q, from the surroundings *to* the mixed layer is, therefore,

$$q = -k\frac{T_1}{d}[\gamma_t\theta(y, 0, t) + \gamma_b\theta(y, -1, t)], \quad (49)$$

and if we use the lowest-order result for $\kappa = 0$ given in (40), we find the net heat flux

$$q = k\frac{T_1 u_{yy}}{d\tau}. \quad (50)$$

In expressions (47)–(50), k represents the thermal conductivity of water.

The relation (50) shows that there is a net transfer of heat to the mixed layer where there is upwelling and a minimum of surface current in the windward direction; and a net heat transfer out of the mixed layer where there is downwelling and a maximum of the surface current. At the order represented in (50), the horizontally averaged heat transfer vanishes, but if one goes to the next order, the net heat transfer is found to be proportional to $\overline{u_{yy}^2}$, consistent with (46).

When case II ($\gamma \to 0$) applies, the form of the velocity field is the same as for case I, so Figs. 4 and 5 are relevant. However, θ is now u/τ, which is larger than for case I, where $\theta \propto u_{yy}$, because we have assumed $\partial/\partial y$ to be small. The horizontally averaged convective heat flux in this case is

$$-\overline{w\theta} = \overline{uu_{yy}}P(z)/\tau, \quad (51)$$

and the net heat flux from the surroundings to the mixed layer is

$$q = -\frac{k\gamma T_1 u}{d}. \quad (52)$$

The same qualitative remarks made above for case I apply here as well.

Let us consider the estimates provided by the above theory for a particular example. Suppose we consider a mixed layer having a depth of 40 m, subject to a wind speed $U_a = 10$ m s^{-1}, so $u_* \approx 1$ cm s^{-1}; and a temperature variation from the surface to the base of the mixed layer of $T_1 = 0.5$ K. The latter yields a value of $\Delta\rho/\rho$ of about 10^{-4} when a coefficient of thermal expansion $\beta \sim 2 \times 10^{-4}$ is used. Then, $S = R_*^2(gd/u_*^2) \times 10^{-4} \sim 400R_*^2$. Suppose α_t and γ_t are negligible compared to α_b and γ_b, and suppose $\alpha_b = 0.24$. The destabilizing parameter

$$R = R_*^2\frac{d}{u_*}\frac{\partial U_S^*}{\partial z}(0),$$

on using (9).

Various estimates give R_* between 5 and 50, with a reasonable value being 15. In this case, $\gamma > \gamma_S$, so that case I is appropriate. Instability obtains in this case when

$$R > R_c \approx 120 + 22\sqrt{S},$$

where we have used the values for the example to evaluate R_c. This may be written

$$\frac{\partial U_S}{\partial z}(0) > 120\frac{u_*}{dR_*^2} + 440\frac{u_*}{dR_*}.$$

Replacing the wave field by a monochromatic wave train gives

$$\frac{\partial U_S}{\partial z} = 2\epsilon^2\omega,$$

where ϵ is the wave slope measure (wave amplitude times wavenumber, or π times the wave height divided by wavelength), and ω is the wave frequency. The latter may be estimated as g/U_a, in which case the stability condition is on the wave slope, $\epsilon > 0.06$, where we have inserted the numerical values (including $R_* = 15$) for the example. The critical wavenumber in this case is $k_c \approx 0.13$, which is very small.

In the case $S = 0$ (corresponding to $T_1 = 0$), a repetition of the above procedure leads to the stability condition $\epsilon > 0.62\sqrt{u_*/d} \approx 0.01$ on again using $R_* = 15$. Thus, only very weak waves are required, and so typical wind-generated seas are expected to be substantially supercritical in the absence of stabilizing temperature gradients. For this example, we find $k_c = 1.1$ from the small-α theory when $S = 0$, and this agrees very well with the numerical prediction from the partial differential equations of linear stability theory.

As S increases, the length of the marginally unstable mode ("windrow" spacing) increases. Small temperature differences over the mixed layer can result in large values of S for a mixed layer that is tens of meters deep. In this case, the nominal windrow spacing calculated

in this way increases with the one-quarter root of S, and the slope of the surface waves needed to cause instability increases with the square root.

7. Summary

We have considered the Craik–Leibovich theory for Langmuir circulations and have introduced new boundary conditions to account for the transmission of stress at the top and bottom of the mixed layer. These are mixed boundary conditions involving parameters that are small in many cases of oceanographic interest; we have denoted these parameters by α_t and α_b at the top and bottom of the mixed layer, respectively. We have also introduced mixed boundary conditions for the temperature, with similar small parameters, γ_t and γ_b. In section 2 we described the derivation and the physical basis for these boundary conditions and estimated values for the parameters α_t, α_b, γ_t, γ_b. With these new boundary conditions we have examined the linear stability of the basic state of structureless equilibrium.

Previous treatments of the Craik–Leibovich theory using the CSM, where a constant stress is assumed at the top and bottom of the mixed layer (equivalent to setting $\alpha_t = \alpha_b = 0$ in the present work), had the unfortunate property that the first motions to become unstable were of infinite wavelength. By taking a positive value for $\alpha = \alpha_t + \alpha_b$, we have made finite the wavelength of the first unstable motions. Further, for small values of α, $k_c \propto \alpha^{1/4}$, where k_c is the critical wavenumber to which the first instability arises as R increases through R_c. We expect that the neglect of α_b is less appropriate in modeling the stress transmission than the neglect of α_t—however, each of these parameters plays the same mathematical role in fixing a finite horizontal length scale for the motions. Indeed, to leading order α_t and α_b occur in the expression for the linear growth rate only as the sum $\alpha_t + \alpha_b$. We have analyzed the problem in the physically realistic limit as $\alpha \to 0$ by expanding the solution as a power series in k. The results of this analysis are described in section 4.

Such an expansion indicates that, according to the values of parameters related to the temperature field, there are three cases for the linear stability problem. The first (I) applies when the parameter $\gamma = \gamma_t + \gamma_b$ is not small and is analogous to the problem of Rayleigh–Bénard convection between poorly conducting boundaries. In this case the convective motions for R just above R_c are steady. The other two possibilities [II(S) and II(H)] have not previously been examined in either this, or in analogous, problems. These two cases apply for small values of the parameter γ; that is, when the temperature boundary condition is almost constant flux. Case II(S) applies when the basic state has a slight density stratification, while case II(H) applies for larger values of the stratification parameter, S. The former, like case I, produces steady convective motions, although with greater temperature variations than I. The latter yields oscillatory convection. Deciding which case applies for given values of the parameters is a nontrivial matter. In section 4e we described a way to estimate the appropriate case, which is valid in the physically interesting limits as $\alpha, \gamma \to 0$. We have not explored the interactions between the different modes of instability when the parameters are near the boundary between cases II(S) and II(H).

The new boundary conditions on the stress successfully overcome the previous problem of infinite-wavelength motions predicted at onset by the CSM. When $\alpha = 0$ and $R > R_0$, the mode with the greatest linear growth rate has finite wavelength [$\propto (R - R_0)^{-1/2}$], but *nonlinear* simulations (Chapman and Proctor 1980) indicate that in spite of this, motions cascade to the largest horizontal scale available. For the present model, the largest horizontal scales are stabilized, and we therefore anticipate a nonlinear cascade only up to some finite cell wavelength, comparable to that of the linearly most unstable mode.

In section 5 we gave the nonlinear partial differential equation governing the steady motions just above onset for cases I and II(S). In each case the equation takes the same form, but with different coefficients. It governs only the perturbation, u, to the wind-directed velocity; the temperature field and the streamfunction can be constructed from u and its derivatives. We defer a description of the solutions to this nonlinear partial differential equation to a later date.

The small-k expansion, applied for physically plausible values of parameters for the Langmuir circulation problem, yields a critical wavenumber $k_c \approx 1$. Although this value might seem inconsistent with an analysis that assumes k to be small, we find a posteriori agreement with a solution of the full linear stability problem obtained from (19). For example, at the end of the previous section we deduced a value $k_c = 1.1$ for an unstratified basic state with $\alpha_t = 0$ and $\alpha_b = 0.24$. The solution of the full stability problem, making no assumption about the size of k, yields $k_c = 1.02$, which differs from the small-k result by less than 10%. Other features of the solution, not just the critical wavenumber, are in equally good agreement.

Acknowledgments. This work was supported by NSF OCE-90-17882, ONR N00014-92-J-1547, AFOSR-89-0226, and NSF AM-88-14553.

APPENDIX

Algebraic Details

a. Calculation of the growth rate: Case I

For the purpose of the linear-stability calculation we may take $u_0 = 1$. Then at $O(k^1)$ in the linearization of (19),

$$D^4\psi_1 = -R_0,$$

subject to the boundary conditions $D^2\psi_1 = \psi_1 = 0$ on $z = 0, -1$. The solution is

$$\psi_1 = -R_0(z^4/24 + z^3/12 - z/24).$$

At $O(k^2)$ the value of σ_2 is determined from a solvability condition on the equation for u_2. We have

$$-\sigma_2 + D^2u_2 = 1 + \psi_1,$$

subject to the boundary conditions $Du_2 = 0$ on $z = 0, -1$. Integrating this equation with respect to z and applying the boundary conditions on u_2 gives

$$-\sigma_2 = \int_{-1}^{0} (1 + \psi_1)dz = 1 - R_0/120.$$

We choose $R_0 = 120$ (Nield 1967) so that the growth rate is of order k^4; that is, $\sigma_2 = 0$. Then

$$u_2 = -z^6/6 - z^5/2 + 5z^3/6 + z^2/2 - 1/56,$$

and we have chosen the constant of integration so that $\int_{-1}^{0} u_2 dz = 0$.

The leading-order temperature perturbation satisfies

$$\tau D^2\theta_2 = \psi_1,$$

subject to the boundary conditions $D\theta_2 - \gamma_b\theta_2 = 0$ on $z = -1$ and $D\theta_2 + \gamma_t\theta_2 = 0$ on $z = 0$. The solution is

$$\tau\theta_2 = -\frac{z^6}{6} - \frac{z^5}{2} + \frac{5z^3}{6} - \frac{(\gamma_b + 2)(\gamma_t z - 1)}{2(\gamma_t\gamma_b + \gamma)}.$$

We note that for this solution to exist we require the assumption made previously, that $\gamma > 0$.

The equation for ψ_3,

$$D^4\psi_3 = 2D^2\psi_1 - R_0u_2 - R_2 + S\theta_2, \qquad (53)$$

can be solved subject to the boundary conditions that $D^2\psi_3 = \psi_3 = 0$ on $z = 0, -1$. The expression for ψ_3 is quite lengthy and is omitted here.

At $O(k^4)$ we obtain σ_4 from a solvability condition applied to the equation for u_4:

$$-\sigma_4 + D^2u_4 = u_2 + \psi_3, \qquad (54)$$

subject to the boundary conditions

$$Du_4 = -\bar{\alpha}_t \quad \text{on} \quad z = 0, \quad Du_4 = \bar{\alpha}_b \quad \text{on} \quad z = -1.$$

Integrating (54) across the depth of the layer gives

$$\sigma_4 = -\bar{\alpha} + \frac{R_2}{R_0} - \left[\frac{1091}{5544} + \left(\frac{S}{\tau}\right)\frac{691\gamma_t\gamma_b + 2077\gamma + 5544}{665280(\gamma_t\gamma_b + \gamma_t + \gamma_b)}\right],$$

and hence (28).

b. Calculation of the growth rate: Case II(S)

Solving (29) and (30) for u_2 and θ_2 we find

$$u_2 = -z^6/6 - z^5/2 + 5z^3/6 + z^2/2 - 1/56 + u_2',$$

$$\tau\theta_2 = -z^6/6 - z^5/2 + 5z^3/6 + z^2/2 - 1/56 + \tau\theta_2'.$$

Here, u_2' and θ_2' are constants of integration. We may set one (but not both) of these quantities to zero, and choose $u_2' = 0$.

The equation for ψ_3 is again (53), subject to the same boundary conditions as given below (53). As before, we omit the lengthy expression for ψ_3.

At $O(k^4)$ we find the governing equations for u_4 and θ_4 to be

$$\sigma_4u_0 - D^2u_4 = -u_2 - \psi_3,$$

$$\sigma_4\theta_0 - \tau D^2\theta_4 = -\tau\theta_2 - \psi_3.$$

Integrating both equations across the layer and applying the boundary conditions, that $Du_4 = -\bar{\alpha}_t$ on $z = 0$, $Du_4 = \bar{\alpha}_b$ on $z = -1$, $D\theta_4 = 0$ on $z = 0, -1$, we find the two conditions

$$\begin{pmatrix} -1 & -\tau\Sigma \\ -1/\tau & -\tau(1 + \Sigma) \end{pmatrix}\begin{pmatrix} \sigma_4 \\ \theta_2' \end{pmatrix} = \begin{pmatrix} 1091/5544 - R_2/120 + \bar{\alpha} \\ 1091/5544 - R_2/120 \end{pmatrix}.$$

We note that the matrix has determinant $\tau - \Sigma(1 - \tau)$, which is nonzero (in fact, negative) by our original assumption of a steady bifurcation, so a unique solution of this equation exists. In particular,

$$\left(1 + \frac{\Sigma(\tau - 1)}{\tau}\right)\sigma_4 = -\bar{\alpha}(1 + \Sigma) + \frac{R_2}{120} - \frac{1091}{5544},$$

and hence (33).

c. Calculation of the growth rate: Case II(H)

In case II(H), where $(1 - \tau)\Sigma > \tau$, the basic state becomes unstable to oscillatory convection. An analysis similar to those presented above yields $\sigma = \sigma_r \pm i\sigma_i$, where to $O(k^4)$

$$\sigma_r = -\frac{\alpha}{2} + \frac{R - R_H}{240}k^2 - \frac{k^4}{11088}\{\Sigma(1 - \tau)(31 - 530\tau) + (1 + \tau)[530\tau + 1091]\}, \qquad (55)$$

and

$$\sigma_i = \omega k^2 + \omega^{-1}\left\{\frac{-(R - R_H)}{240}k^2 + \frac{\tau\alpha}{2}(1 + \Sigma) + \frac{k^4}{11088}\right.$$

$$\times [\tau(\tau + 1)(530\tau + 1091) - \Sigma\tau(1 - \tau)$$
$$\times (499\tau + 1621) - 31\Sigma^2\tau(\tau - 1)^2]\Big\}.$$

REFERENCES

Busch, N. E., 1977: Fluxes in the surface boundary layer over the sea. *Modelling and Prediction of the Upper Layers of the Ocean,* E. B. Kraus, Ed., Pergamon, 72–91.

Chapman, C. J., and M. R. E. Proctor, 1980: Nonlinear Rayleigh–Bénard convection between poorly conducting boundaries. *J. Fluid Mech.,* **101,** 759–782.

——, S. Childress, and M. R. E. Proctor, 1980: Long wavelength thermal convection between nonconducting boundaries. *Earth Planet. Sci. Lett.,* **51,** 362–369.

Cox, S. M., S. Leibovich, I. M. Moroz, and A. Tandon, 1992a: Nonlinear dynamics in Langmuir circulations with O(2) symmetry. *J. Fluid Mech.,* **241,** 669–704.

——, ——, ——, and ——, 1992b: Hopf bifurcations in Langmuir circulations. *Physica,* **59D,** 226–254.

Craik, A. D. D., 1977: The generation of Langmuir circulations by an instability mechanism. *J. Fluid Mech.,* **81,** 209–223.

——, and S. Leibovich, 1976: A rational model for Langmuir circulations. *J. Fluid Mech.,* **73,** 401–426.

Depassier, M. C., and E. A. Spiegel, 1982: Convection with heat flux prescribed on the boundaries of the system. I. The effect of temperature dependence of material properties. *Geophys. Astrophys. Fluid Dyn.,* **21,** 167–188.

Gertsberg, V. L., and G. I. Sivashinsky, 1981: Large cells in nonlinear Rayleigh–Bénard convection. *Prog. Theor. Phys.,* **66,** 1219–1229.

Huang, N. E., 1979: On surface drift currents in the ocean. *J. Fluid Mech.,* **91,** 191–208.

Kantha, L. H., 1977: Note on the role of internal waves in thermocline erosion. *Modelling and Prediction of the Upper Layers of the Ocean,* E. B. Kraus, Ed., Pergamon, 173–177.

——, and O. M. Phillips, 1976: On turbulent entrainment at a stable density interface. *J. Fluid Mech.,* **79,** 753–768.

Knobloch, E., 1990: Pattern selection in long-wavelength convection. *Physica,* **41D,** 450–479.

Langmuir, I., 1938: Surface motion of water induced by wind. *Science,* **87,** 119–123.

Leibovich, S., 1977a: On the evolution of the system of wind drift currents and Langmuir circulations in the ocean. Part 1. Theory and averaged current. *J. Fluid Mech.,* **79,** 715–743.

——, 1977b: Convective instability of stably stratified water in the ocean. *J. Fluid Mech.,* **82,** 561–581.

——, 1980: On wave–current interaction theories of Langmuir circulations. *J. Fluid Mech.,* **99,** 715–724.

——, 1985: Dynamics of Langmuir circulations in a stratified ocean. *The Ocean Surface,* Y. Toba and H. Mitsuyasu, Eds., Reidel, 457–464.

——, and K. Radhakrishnan, 1977: On the evolution of the system of wind drift currents and Langmuir circulations in the ocean. Part 2. Structure of the Langmuir vortices. *J. Fluid Mech.,* **80,** 481–507.

——, S. Lele, and I. M. Moroz, 1989: Nonlinear dynamics in Langmuir circulations and in thermosolutal convection. *J. Fluid Mech.,* **198,** 471–511.

Lele, S. K., 1985: Some problems in hydrodynamic stability arising in geophysical fluid dynamics. Ph.D. thesis, Cornell University, 302 pp.

Moroz, I. M., and S. Leibovich, 1985: Competing instabilities in a nonlinear model for Langmuir circulations. *Phys. Fluids,* **28,** 2050–2061.

Nield, D. A., 1967: The thermohaline Rayleigh–Jeffreys problem. *J. Fluid Mech.,* **29,** 545–558.

Niiler, P. P., and E. B. Kraus, 1977: One-dimensional models of the upper ocean. *Modelling and Prediction of the Upper Layers of the Ocean,* E. B. Kraus, Ed., Pergamon, 143–172.

Phillips, O. M., 1977: *The Dynamics of the Upper Ocean,* 2d ed., Cambridge University Press, 336 pp.

Pollard, R. T., and R. C. Millard, 1970: Comparison between observed and simulated wind-generated inertial oscillations. *Deep-Sea Res.,* **17,** 813–821.

Proctor, M. R. E., 1981: Planform selection by finite-amplitude thermal convection between poorly conducting slabs. *J. Fluid Mech.,* **113,** 469–485.

Roberts, A. J., 1985: An analysis of near-marginal, mildly penetrative convection with heat flux prescribed on the boundaries. *J. Fluid Mech.,* **158,** 71–93.

Sivashinsky, G. I., 1982: Large cells in nonlinear Marangoni convection. *Physica,* **4D,** 227–235.

——, 1983: On cellular instability in the solidification of a dilute binary alloy. *Physica,* **8D,** 243–248.

Smith, J., R. Pinkel, and R. A. Weller, 1987: Velocity structure in the mixed layer during MILDEX. *J. Phys. Oceanogr.,* **17,** 425–439.

Sparrow, E. M., R. J. Goldstein, and V. K. Jonsson, 1964: Thermal instability in a horizontal fluid layer: Effect of boundary conditions and non-linear temperature profile. *J. Fluid Mech.,* **18,** 513–528.